Isothermal aggregation of Bi atoms embedded in a soda borate glass: Coarsening of liquid nanodroplets and atomic diffusion

G. Kellermann[1,2,*] and A. F. Craievich[3]
[1]*Laboratório Nacional de Luz Síncrotron, C.P. 6192, 13084-971 Campinas SP, Brazil*
[2]*Instituto de Física "Gleb Wataghin," UNICAMP, C.P. 6165, 13083-970 Campinas SP, Brazil*
[3]*Instituto de Física, USP, C.P. 66318, CEP 05315-970, São Paulo SP, Brazil*
(Received 8 August 2002; revised 26 November 2002; published 7 February 2003)

The process of nucleation and growth of liquid Bi nanodroplets embedded in a soda borate glass submitted to isothermal annealing at different temperatures was studied by small-angle x-ray scattering (SAXS) and transmission-electron microscopy. The experimental results indicate that the formation and growth of Bi droplets occur in two successive stages after a short incubation period. The first is characterized by the nucleation and growth of spherical droplets promoted by atomic diffusion and aggregation of isolated Bi atoms and the second one by a subsequent droplet coarsening. The experimental functions describing the time variation of the droplet average radius and density number at advanced stages of the growth process agree with the classical Lifshitz-Slyozov-Wagner (LSW) theory. However, the radius distribution was demonstrated to be well described by a log-normal function thus differing from the prediction of the LSW model. The atomic diffusion coefficient of Bi was determined from SAXS results for several annealing temperatures and, from it, the activation energy for the diffusion process was inferred.

DOI: 10.1103/PhysRevB.67.085405 PACS number(s): 61.10.Eq, 66.10.Cb, 81.10.Jt

I. INTRODUCTION

Nanometer-sized metallic particles have attracted the interest of many scientists due to their potential uses as catalysts and heat-exchange materials. Due to their singular optical properties, particular interest was addressed to composite materials consisting of metallic clusters embedded in glass matrices. A detailed review of the properties and characterization techniques of metal nanoclusters was reported by Gonella and Mazzoldi.[1]

This is a study of the kinetics of formation and growth of liquid Bi clusters embedded in a soda borate glass. Initially homogeneous and Bi-doped glass samples are studied by *in situ* small-angle x-ray scattering (SAXS) during isothermal annealing at temperatures close to the soda borate glass transition ($\sim$800–850 K). The annealing temperatures being well above the melting temperature of bulk Bi crystals ($T_m = 544.4$ K), the spherical clusters are in the liquid state from the first stages until the end of their growth. From the results of SAXS experiments, the radius distribution function, the time dependence of the average radius, the radius dispersion, and the number density of the liquid nanodroplets are determined. These experimental results are compared to those predicted by the classical theories of growth of spherical droplets embedded in a supersaturated matrix.

In addition, the coefficients of diffusion of Bi atoms through the glass matrix are determined from SAXS results at several temperatures and, from this, the energy of activation for the diffusion process is evaluated. Complementary measurements of transmission-electronic microscopy (TEM) and x-ray-absorption near-edge structure (XANES) are performed in order to verify the shape of the Bi nanoclusters and estimate the total concentration of Bi in the glass, respectively.

This study is a detailed *in situ* characterization, at high temperature, of the formation of a Bi liquid droplet-soda borate glass nanocomposite. After cooling down to room temperature, this system transforms into a Bi nanocrystal-glass nanocomposite. The structure and melting behavior of these Bi nanocrystals embedded in a glass matrix have recently been investigated and published elsewhere.[2]

II. EXPERIMENT

The starting raw materials were Na_2CO_3, B_2O_3, Bi_2O_3, and SnO. SnO was added as a reducing agent for Bi_2O_3. This mixture was melted in an electrical furnace under vacuum (10^{-1} mbar) at 1313 K. A $28Na_2O$-$72B_2O_3$ glass containing dispersed Bi atoms was obtained by fast quenching of the melted glass down to room temperature using the splat-cooling technique. The obtained 100-μm-thick glass plates were homogeneous and transparent to visible light. The quenching procedure prevents glass crystallization and suppresses, or strongly reduces, the formation of Bi clusters during cooling. The SAXS intensity produced by the glass samples was measured *in situ*, during isothermal annealing at temperatures ranging from 803 up to 843 K in a specially designed high-temperature cell.[3] After isothermal annealing, the sample was cooled down to room temperature and studied by TEM.

The SAXS experiments were performed at the SAS beamline of the National Synchrotron Light Laboratory (LNLS), Campinas, Brazil.[4] The SAXS intensity was recorded using a one-dimension gas x-ray position-sensitive detector. X-ray monitors placed before and after the sample measured the intensity of the incoming and transmitted x-ray beam intensity in order to determine the sample attenuation. SAXS spectra were normalized to equivalent intensities of the direct beam to compensate for the continuous decrease in the emission of the synchrotron source. The SAXS intensity was determined as a function of the modulus of the scattering

vector $q=(4\pi \sin\theta)/\lambda$, λ being the wavelength of the x-ray beam ($\lambda=1.61$ Å) and θ half of the scattering angle. The parasitic scattering was subtracted from the total SAXS intensity. Because of the small area of the cross section of the transmitted x-ray beam at the detection plane and the narrow resolution slit used for the detector, the SAXS curves were essentially free from smearing effects. The SAXS intensity was determined in absolute units by using water as a standard.[5]

The TEM study was performed at LME/LNLS, Campinas, Brazil, using a JEM-3010 UHR microscope operating at 300 kV at room temperature. The glass containing the Bi nanocrystals (solidified Bi droplets) was very finely grinded and mixed with isopropanol (100 mg of glass per ml of alcohol). The mixture was maintained in an ultrasonic bath during 10 min and then dropped on a 30-Å carbon film deposited on a cupped grid. After drying, the very thin glass grains, well adhered to the grid, were observed in the microscope.

III. CLASSICAL THEORY OF DROPLET COARSENING

A. Basic aspects

The formation of a second phase consisting of nanoclusters embedded in an supersaturated homogeneous matrix containing doping atoms starts by a nucleation stage and is followed by a further cluster growth promoted by the diffusion and aggregation of initially isolated doping atoms. This mechanism is named ''nucleation and growth.'' According to the model proposed by Lifshitz-Slyosov[6] and Wagner[7] (LSW), when the supersaturation of the doping element in the matrix becomes small, *spherical clusters* with a radius R smaller than a critical radius R_c start to dissolve while those with radii larger than R_c still grow. This is consequence of the driving force for coarsening that promotes the decrease of the area of the interface between the clusters and the matrix phase thus reducing the total interface energy. The cluster radius distribution $N(R,t)$ for different times t of isothermal annealing during the coarsening regime predicted by the LSW model is independent of the initial size distribution $N(R,0)$ and is given by[6]

$$N(R,t)=f(t)\frac{4(R/R_c)^2}{9}\left(\frac{3}{3+R/R_c}\right)^{7/3}\left(\frac{3/2}{3/2-R/R_c}\right)^{11/3}\times\exp\left(\frac{-R/R_c}{3/2-R/R_c}\right), \quad (1)$$

where $f(t)$ is a function of the annealing time only. During the coarsening stage R_c coincides with the cluster average radius $\langle R\rangle$. The cluster average radius $\langle R\rangle(t)$, the concentration of solute atoms in the matrix $c(t)$, and the number density of clusters $n(t)$ are time-dependent functions. The density number can be determined as $n(t)=\int N(R,t)dR$.

During the coarsening stage, $\langle R\rangle(t)$ increases for increasing times while $n(t)$ progressively decreases. Quantitatively, according to the LSW model, the time dependence of $\langle R\rangle\times(t)$, $n(t)$, and $c(t)$ satisfy the following equations:[6–8]

$$\langle R\rangle^3(t)=\langle R_0\rangle^3+\kappa(t-t_0) \quad (t\geqslant t_0), \quad (2)$$

$$n^{-1}(t)=n_0^{-1}+\beta(t-t_0) \quad (t\geqslant t_0), \quad (3)$$

$$c(t)=c_e+\chi^{-1/3}(t-t_0)^{-1/3} \quad (t\geqslant t_0), \quad (4)$$

where $\langle R_0\rangle$ and n_0 are the average radius and number density of the clusters, respectively, at the starting time for coarsening $t=t_0$ and c_e is the concentration of solute atoms (number per unit volume) in the matrix at equilibrium. An equation equivalent to Eq. (4) can be written in terms of the volume fraction of the new phase,[9]

$$\varphi(t)=\varphi_e-\chi'^{-1/3}(t-t_0)^{-1/3} \quad (t\geqslant t_0), \quad (5)$$

where φ_e is the volume fraction of the new phase at equilibrium. Equations (2)–(5) hold for annealing times $t\geqslant t_0$. The equations derived from the LSW model apply to *dilute* two-phase systems composed of spherical clusters occupying a low fraction of the total volume.

B. Determination of the atomic diffusion coefficient from SAXS results

The four rate parameters κ, β, χ, and χ' in Eqs. (2)–(5), respectively, are related to the atomic diffusion coefficient D of the solute as follows:[6–9]

$$\kappa=\frac{8\sigma\nu^2c_eD}{9kT}, \quad (6)$$

$$\beta=\frac{4\sigma c_e\nu D}{(c_i-c_e)kT}, \quad (7)$$

$$\chi=\frac{D(kT)^2}{9\sigma^2c_e^2\nu}, \quad (8)$$

$$\chi'=\left(\frac{1/\nu-c_e}{1-\varphi_e}\right)^3\chi, \quad (9)$$

where σ is the free energy per unit of area of the interface between clusters and the matrix, ν the atomic volume of the solute, c_i the initial concentration of solute in the matrix, k the Boltzmann constant, and T the absolute temperature. Since the parameters σ and c_e are in many cases not known, Eqs. (6)–(9) cannot generally be used to determine the diffusion coefficient D.

By combining Eqs. (6) and (8) we have

$$\kappa^2\chi=\left(\frac{4}{9}\nu D\right)^3$$

and thus

$$D=\frac{9}{4\nu}(\kappa^2\chi)^{1/3}.$$

Finally, using Eq. (9) and assuming that $[(1/\nu)-c_e]\approx 1/\nu$, we have

$$D=\frac{9(1-\varphi_e)}{4}(\kappa^2\chi')^{1/3}. \quad (10)$$

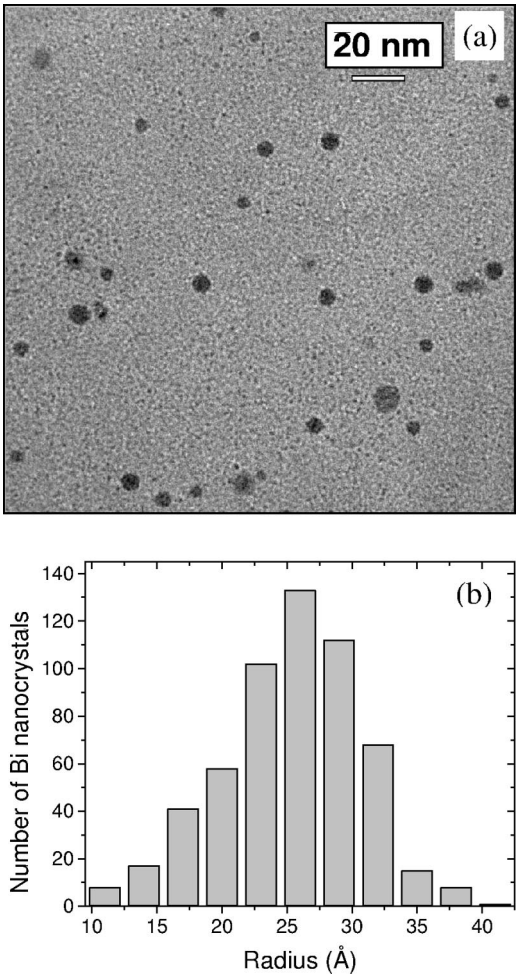

FIG. 1. (a) Transmission-electron microscopy bright field image corresponding to a thin sample annealed 2 h at 843 K. (b) Histogram of droplet radii.

If, beside c_i, c_e, φ_e, and T, also D, σ, and ν are approximately constant during the whole coarsening process, the rate parameters κ, β, χ, and χ' [Eqs. (2)–(5) respectively] are expected to have *constant values along the whole coarsening process*, i.e., under the mentioned conditions, the LSW theory predicts that during the cluster coarsening process $\langle R\rangle^3(t)$ and $n^{-1}(t)$ are linear functions of the annealing time and $c(t)$ and $\varphi(t)$ are linear functions of $(t-t_0)^{-1/3}$. Since the relevant parameters φ_e, κ, and χ' are easily determined from SAXS results in an absolute scale, Eq. (10) can be applied to the determination of D without the explicit knowledge of σ and c_e.

IV. RESULTS AND DISCUSSION

A. Transmission-electron microscopy

The TEM image given in Fig. 1(a) shows Bi nanocrystals embedded in the soda borate glass matrix corresponding to a sample held during 2 h at 843 K and cooled down to room temperature. The image demonstrates that Bi nanocrystals have a nearly spherical shape. Figure 1(b) shows the histogram of the number of Bi nanocrystals as a function of their radii. The analysis of the TEM image indicates a single-mode radius distribution function [Fig. 1(b)].

The average nanocrystal radius $\langle R\rangle$ and the relative radius dispersion $\sigma_R/\langle R\rangle$ are (25 ± 2) Å and (0.21 ± 0.01), respectively. The histogram was obtained from the measured diameters of 560 nanocrystals corresponding to different grains of the glass-Bi nanocrystals composite. The estimated resolution limit for size determination was 18 Å (minimum measurable radius: 9 Å). The diameter of each nanocrystal was determined from the diameter of a circle that best fit the perimeter of their projected images.

In order to compare the radius distribution function derived from the TEM image with those from SAXS experiments, we have considered that the radius distribution of Bi nanocrystals obtained by TEM at room temperature is essentially the same as the radius distribution of liquid Bi nanodroplets in the precursor sample just before cooling. This is a reasonable assumption because the temperature range of the liquid-to-crystal transition is well below the softening temperature of the glass matrix.[2]

B. Small-angle x-ray scattering

1. Formation and growth of the new phase

We wish to characterize the mechanisms of formation and growth, during isothermal annealing, of a dilute and isotropic set of spherical Bi droplets embedded in an initially homogeneous Bi supersaturated glass. We remind the reader that the Bi clusters are in a liquid state because the annealing temperatures ($\approx$800–850 K) are well above the melting temperature of Bi nanocrystals.[2] The shape of the liquid droplets is expected to be spherical as a consequence of the dominant effect of surface tension. As will be described below, under these conditions the SAXS intensity is a particularly simple function of the modulus of the scattering vector.

In general, the scattering intensity in absolute units, or scattering power, is given by the differential scattering cross section $d\Sigma/d\Omega$. For a dilute set of spherical droplets with constant electron density ρ_p embedded in a homogeneous matrix with a constant electron density $\langle\rho\rangle$, the scattering power is given by[10]

$$\frac{d\Sigma}{d\Omega}(q)=r_0^2(\Delta\rho)^2\left(\frac{4\pi}{3}\right)^2\int_0^\infty N(R)P(q,R)R^6dR, \quad (11)$$

where $\Delta\rho=\rho_p-\langle\rho\rangle$ and $N(R)dR$ is the number of droplets per unit volume with radii between R and $R+dR$. $r_0=0.28179\times10^{-14}$ m is the classical electron radius and $P(q,R)$ is the normalized form factor for a sphere defined by[10]

$$P(q,R)=\left[3\frac{\sin(qR)-qR\cos(qR)}{(qR)^3}\right]^2. \quad (12)$$

An additional and essentially q-independent contribution to the scattering intensity produced by electron-density fluctuations in the matrix is experimentally determined by using Porod plots[10] and subtracted from the total scattering intensity.

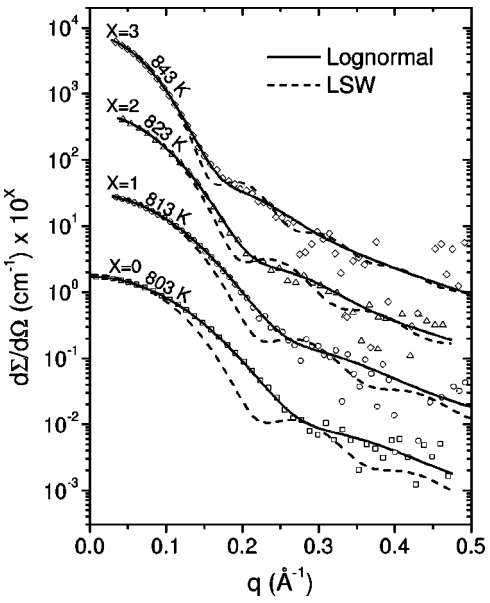

FIG. 2. Scattering power corresponding to samples annealed during 100 min at the indicated temperatures. Modeled curves using the functions defined by Eqs. (1) and (13) are also plotted. The curves from $x=1-3$ are multiplied by increasing powers of 10 for clarity.

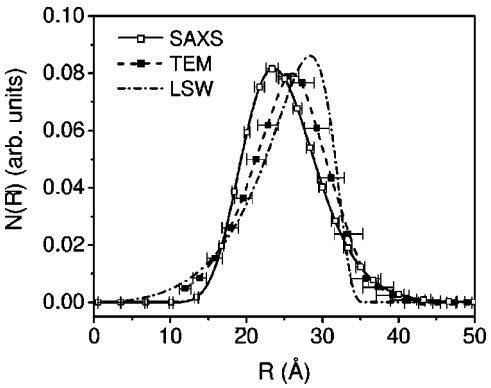

FIG. 3. Nanocrystal radius distributions $N(R)$ corresponding to a sample annealed at 843 K during 2 h. These functions were obtained from (i) an experimental SAXS curve assuming a log-normal radius distribution and (ii) the TEM histogram displayed in Fig. 1(b). Both radius distribution functions yield the same average radius ($\langle R\rangle=25$ Å). The third curve is the radius distribution function predicted by the LSW model [Eq. (1)] for same average radius. The areas under the curves are normalized to unity.

According to our already mentioned TEM results, the assumptions regarding the dilute nature of the solution and the spherical shape of the clusters apply to the system that we study here. The Bi concentration in the samples, determined from absorption x-ray spectroscopy (XANES) measurements, is of the order of 10^{-5} mol/cm^3. The electron densities of the initial glass matrix $\langle\rho\rangle$ and of Bi nanodroplets ρ_p were determined from the known nominal composition and mass density of the glass and from the mass density of bulk melted Bi, respectively. Due to the decreasing trend in the number of Bi atoms dissolved in the glass matrix, a variation in the difference between the electron density of Bi nanodroplets and the glass matrix ($\Delta\rho=\rho_p-\langle\rho\rangle$) is expected. Because of the small Bi concentration, this difference is only very slightly modified during the whole annealing process and so it was assumed to maintain a constant value.

The experimental SAXS intensity curves at advanced stages of thermal annealing were modeled assuming the radius distribution predicted by LSW theory, Eq. (1). As an alternative attempt, the scattering intensity curves were modeled assuming a log-normal radius distribution function defined by

$$N(R)=\frac{n}{\sqrt{2\pi e^{w^2}}wr}\exp\left\{-\frac{1}{2}\frac{[\ln(R/r)]^2}{w^2}\right\}, \qquad (13)$$

where r, w, and n are fitting parameters, n being the droplet number density.

The scattering power (SAXS intensity in absolute units) corresponding to 100 min of isothermal annealing and the best modeled curves for both size distribution functions [Eqs. (1) and (13)] are plotted in Fig. 2. The best fit using Eq. (1) leads to a function that exhibits significant deviations from the experimental results. On the other hand, the curves obtained by assuming a log-normal radius distribution function [Eq. (13)] fitted very well the experimental data except at the very beginning of the process.

In order to compare the radius distribution functions derived from SAXS and TEM results, we have focused on a particular sample annealed during 2 h at 843 K. In Fig. 3 the log-normal radius distribution function [Eq. (13)] determined from a SAXS experiment and that deduced from a TEM image [Fig. 1(b)] are plotted together with the distribution predicted by the LSW model [Eq. (1)] for $\langle R\rangle=25$ Å. The presented results indicate that even though the radius distribution determined from SAXS and TEM analyses are not identical, the average radius obtained using both methods is the same ($\langle R\rangle=25$ Å). The error bars are ±0.1 Å and ±2 Å for SAXS and TEM, respectively. The relative dispersions of the distribution function $N(R)$ determined from SAXS and TEM results are $\sigma_R/\langle R\rangle=0.190\pm0.005$ and $\sigma_R/\langle R\rangle=0.21\pm0.01$, respectively. This indicates that both techniques lead to average radius and radius dispersion in very good agreement. The differences in the distribution profile may be due to the rather low sampling in TEM analysis and/or to the inherent approximation associated to the use of a log-normal function for the analysis of SAXS results.

As it can be seen in Fig. 3, the shape of the radius distribution function $N(R)$ determined from SAXS results is not identical to that predicted by the LSW model. In fact, deviations of the experimental radius distribution from that predicted by the LSW theory [Eq. (1)] have already been reported in a number of previous investigations.[8,9] The reported deviations may be, at least partially, due to systematic errors associated to the procedure used for size determination. In the present work, the different shape may be also related to the more or less good approximation involved in the assumption of a log-normal function for the radius distribution. However, the structural parameters whose time de-

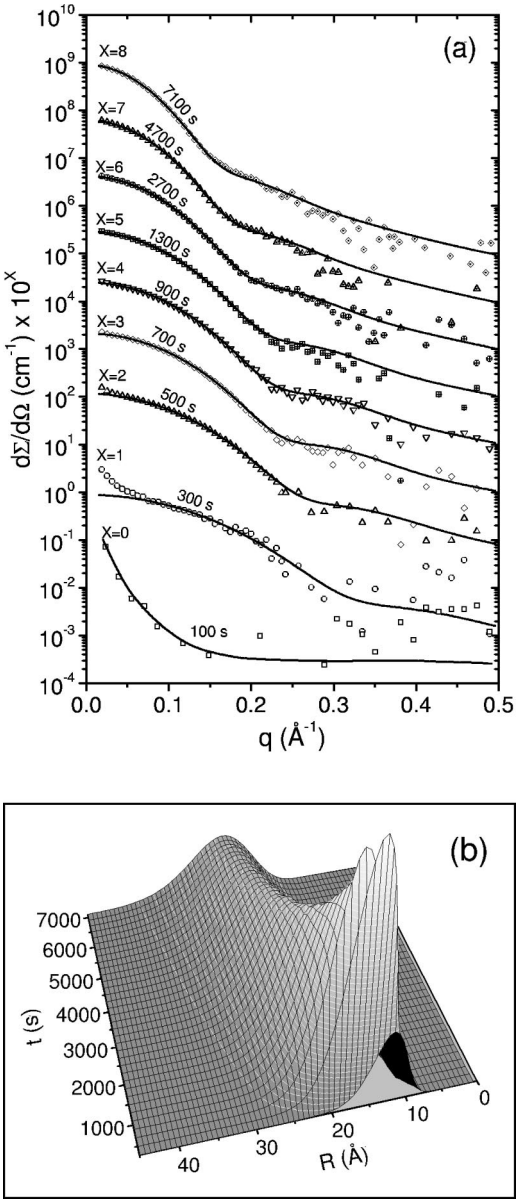

FIG. 4. (a) Scattering power corresponding to a sample annealed at 843 K during the indicated time periods. The continuous line is the modeled function assuming a log-normal radius distribution. The curves from $x=1-8$ are multiplied by increasing powers of 10 for clarity. (b) Radius distribution as a function of the annealing time determined from data plotted in (a).

pendence is used here in order to characterize the mechanism of Bi droplet growth (i.e., $\langle R\rangle$, n, and φ) depend on integrals involving the $N(R)$ function and not on its detailed shape. As we will see in the next section, in spite of the mentioned discrepancy in the profile of the $N(R)$ function, the experimentally observed time dependencies of $\langle R\rangle$, n, and φ agree very well with those predicted by the LSW model.

The scattering power corresponding to different periods of annealing at 843 K and the modeled curves according to Eqs. (11) and (13) are plotted in Fig. 4(a). At the beginning of thermal treatment, corresponding to the induction period, only a very weak and q-independent scattering, except at the very small angles, is observed. The scattering at very small angles is attributed to the existence of a few and rather large Bi clusters in the as-quenched glass. In the above fitting procedure, the data corresponding to very small angles were not considered.

The log-normal distributions $N(R,t)$ associated to the modeled scattering power curves for different annealing times are plotted in Fig. 4(b). The results evidence an initial stage with very fast nucleation and growth of the Bi nanodroplets, indicated by the increase of the area under $N(R,t)$ curves, and a shift of the maximum of the radius distribution toward higher R values. The nucleation and growth period is about 10 min at 843 K and longer at lower temperatures. After this transient period, a continuous reduction in the number of nanodroplets occurs. On the other hand, the maximum of the distribution continuously shifts toward higher R values thus indicating a continuous growth of nanodroplets from the beginning until the end of the coarsening process. The fitting procedure applied to the whole set of scattering curves yielded the time variations in average radius, number density, and relative radius dispersion of nanodroplets, $\langle R\rangle \times(t)$, $n(t)$, and $[\sigma_R/\langle R\rangle](t)$, respectively.

Figure 5(a) displays the dependence of $\langle R\rangle^3$ on the annealing time. After the induction period, a very fast growth of nanodroplets is observed. Later, it follows a stage in which nanodroplets grow at a lower rate until the end of the annealing process. The linear dependence of the experimental $\langle R\rangle^3(t)$ function agrees with the prediction of LSW coarsening theory [Eq. (2)]. As expected, the $\langle R\rangle^3(t)$ growth rate—slope κ—is an increasing function of the temperature.

The function $n^{-1}(t)$ is plotted in Fig. 5(b). The fast increase in the number density of nanodroplets at the beginning of the thermal treatment indicates an initial nucleation stage. Later, a continuous reduction of nanodroplet number density is observed. The linear dependence of $n^{-1}(t)$ on the annealing time also agrees with the prediction of LSW theory [Eq. (3)].

In Fig. 5(c), the ratios $\sigma_R/\langle R\rangle$ are displayed as functions of the annealing time for different annealing temperatures. High values of these ratios are observed at the beginning of the annealing. This is an expected consequence of the continuous nucleation of additional clusters in this stage. As a consequence of the decreasing Bi concentration in the glass matrix, the rate of nucleation decreases and $\sigma_R/\langle R\rangle$ falls to a minimum. After this period, when coarsening starts, $\sigma_R/\langle R\rangle$ increases very slightly and at advanced stages becomes nearly constant. The invariance of $\sigma_R/\langle R\rangle$ with respect to the annealing time in this stage indicates that the radius distribution becomes time independent under scaling of the average nanodroplet radius. During advanced stages of annealing $\sigma_R/\langle R\rangle$ is equal to 0.20, in agreement with the value of 0.21 determined from TEM images and $\sigma_R/\langle R\rangle=0.21$ predicted by LSW theory.

2. Experimental determination of the diffusion coefficient and the energy of activation for Bi diffusion from SAXS results

The volume fraction of the solute phase φ can be determined from the integrated scattering power in reciprocal

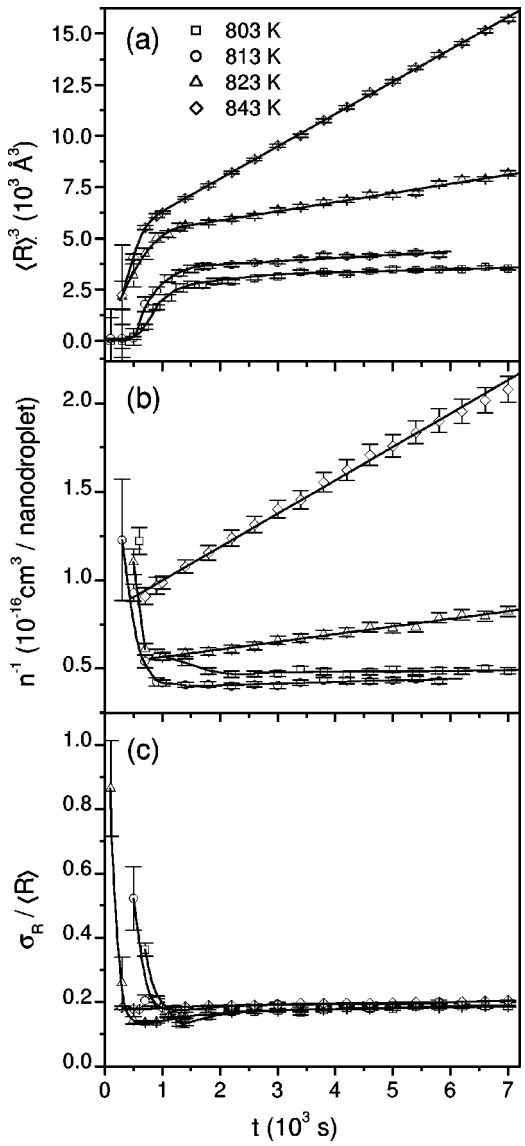

FIG. 5. (a) Cubic average radius $\langle R\rangle^3$, (b) reciprocal number density n^{-1}, and (c) relative radius dispersion $\sigma_R/\langle R\rangle$ as functions of the annealing time at the indicated annealing temperatures.

space Q. For systems in which the new phase is formed by randomly oriented precipitates of any shape, the scattering power is a function of the modulus of the scattering vector q and so the integral Q is given by[10]

$$Q=4\pi\int_{q=0}^{\infty}\frac{d\Sigma}{d\Omega}(q)q^2dq. \tag{14}$$

This integral is related to the volume fraction φ by[10]

$$Q=8\pi^3r_0^2\Delta\rho^2\varphi(1-\varphi). \tag{15}$$

Since in our case the initial Bi concentration in glass is very low (volume fraction $\sim 10^{-4}$), we can safely assume that $\Delta\rho$ is a constant during the whole coarsening process. So, for the new phase occupying the smaller volume fraction, we have

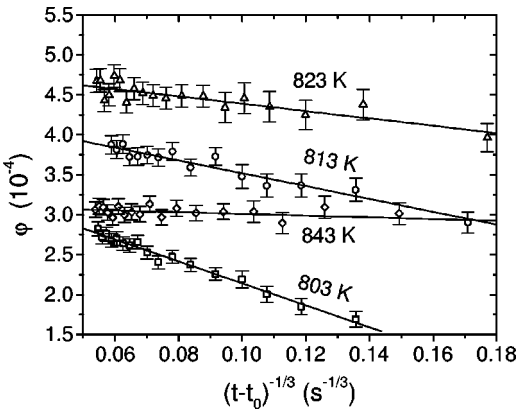

FIG. 6. Total volume fraction of Bi droplets, φ, as a function of $(t-t_0)^{-1/3}$ for the indicated annealing temperatures.

$$\varphi(t)=\frac{1}{2}-\left[\frac{1}{4}-\frac{Q(t)}{8\pi^3r_0^2\Delta\rho^2}\right]^{1/2}. \tag{16}$$

The volume fraction $\varphi(t)$ can also be calculated from the known $N(R,t)$ function

$$\varphi(t)=\frac{4\pi}{3}\int N(R,t)R^3dR. \tag{17}$$

The use of Eq. (16) is preferable because it is a direct calculation from the experimental SAXS curves that yields a more precise $\varphi(t)$ function than that obtained by applying Eq. (17).

Our experimental SAXS results were applied to the determination of the integral Q and, from Eq. (16), the time dependence of the fraction of the total volume occupied by the Bi droplets, $\varphi(t)$, was inferred. A fast increase of $\varphi(t)$ during the first period of annealing indicates that, during this stage, nanodroplets grow mainly by the incorporation of Bi atoms dissolved in the glass that diffuse toward them. After this period $\varphi(t)$ increases at a much smaller rate and is a linear function of $(t-t_0)^{-1/3}$. The $\varphi(t)$ functions versus $(t-t_0)^{-1/3}$ corresponding to the different annealing temperatures are plotted in Fig. 6.

We can see in Figs. 5(a), 5(b), and 6 that the experimental functions $\langle R\rangle^3(t)$ and $n(t)^{-1}$ exhibit a linear dependence on the annealing time and $\varphi(t)$ is a linear function of $(t-t_0)^{-1/3}$, in agreement with the predictions of LSW theory. We stress that this good agreement is actually expected for the studied system because it obeys the basic conditions of validity of the LSW model, i.e., a spherical shape and low total volume fraction of the droplets.

From the slopes of the linear parts of the curves plotted in Figs. 5(a) and 6, we have determined the rate parameters κ and χ', respectively, at different temperatures and, applying Eq. (10), the diffusion coefficients D of Bi through the soda-borate glass were inferred. Since the $\log D$ versus $(1/T)$ plot displayed in Fig. 7 indicates a linear dependence, the diffusion coefficient actually obeys the Arrhenius law:

$$D(T)\propto e^{-E/\mathcal{R}T}, \tag{18}$$

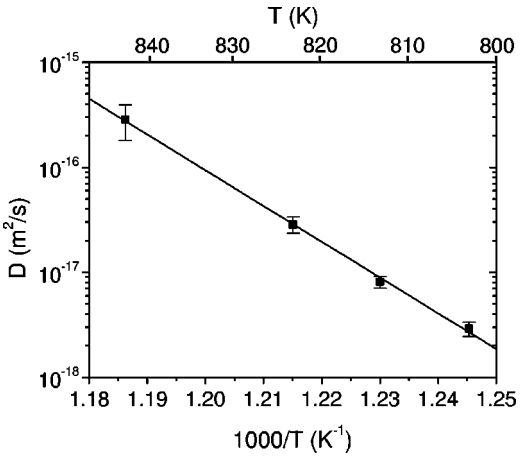

FIG. 7. Arrhenius plot for the diffusion coefficients of Bi atoms through a soda borate glass matrix at different annealing temperatures.

where E is the activation energy for the diffusion process and $\mathcal{R}$ is the gas constant. From the slope of the straight line in a $\log D$ versus $(1/T)$ plot (Fig. 7) the value of the activation energy for Bi diffusion through the soda borate glass $E = (64 \pm 3) \times 10^4$ J mol^{-1} was obtained.

V. CONCLUSION

Our experimental SAXS and TEM results regarding the formation and growth of Bi liquid droplets embedded in the studied Bi-doped soda borate glass evidence a clustering process involving three distinct stages: (i) an initial short incubation stage, (ii) a second fast growth stage during which the size of Bi clusters increases by atomic diffusion and aggregation of isolated Bi atoms, and (iii) a final rather slow stage during which most of the isolated Bi atoms are already aggregated but the nanodroplets still grow by coarsening. The stage of nucleation and growth is characterized by an induction period of the formation of precursor Bi nuclei and by their growth promoted by atomic diffusion of isolated Bi atoms through the glass matrix. This leads to a nanocomposite consisting of a depleted matrix in which spherical nanodroplets with a single-mode radius distribution are homogeneously dispersed.

At more advanced stages of annealing, the time variations of the average radius, the density number of the Bi nanodroplets, and the volume fraction of the new phase are well described by the equations predicted by the LSW model for coarsening. The ratio between the nanodroplets' radius dispersion and their average value is nearly time constant during coarsening as predicted by LSW theory, thus indicating a dynamical scaling property or dynamical self-similarity of the structure. On the other hand, it was demonstrated that the radius distribution is better described by a log-normal function than by the function predicted by the LSW model.

The diffusion coefficients of Bi atoms through the studied soda borate glass during coarsening were quantitatively determined from a set of experimental curves of x-ray scattering power. This evaluation was performed for different annealing temperatures, so from an Arrhenius plot, the activation energy of the diffusion process was also determined. To our knowledge, the present investigation is the first quantitative determination of atomic diffusion coefficients exclusively based on the results of SAXS experiments.

ACKNOWLEDGMENT

The authors thank Edgar D. Zanotto for his helpful suggestions for sample preparation. This work was supported by LNLS, PRONEX, CNPq, and FAPESP.

*Author to whom correspondence should be addressed. Permanent address: Laboratório Nacional de Luz Síncrotron, C.P. 6192, 13084-971 Campinas SP, Brazil. Email address: keller@lnls.br

[1] F. Gonella and P. Mazzoldi, *Handbook of Nanostructured Materials and Nanotechnology* (Academic, New York, 2000).

[2] G. Kellermann and A.F. Craievich, Phys. Rev. B **65**, 134204 (2002).

[3] G. Kellermann, A.F. Craievich, R. Neuenschwander, and T.S. Plivelic, Nucl. Instrum. Methods Phys. Res. B **199**, 112 (2003).

[4] G. Kellermann, F. Vicentin, E. Tamura, M. Rocha, H. Tolentino, A. Barbosa, A.F. Craievich, and I.L. Torriani, J. Appl. Crystallogr. **30**, 880 (1997).

[5] D. Orthaber, A. Bergmann, and O. Glatter, J. Appl. Crystallogr. **33**, 218 (2000).

[6] I.M. Lifshitz and V.V. Slyozov, J. Phys. Chem. Solids **19**, 35 (1961).

[7] C. Wagner, Z. Elektrochem. **4**, 581 (1961).

[8] J. Schmelzer, I. Gutzow, and R. Pascova, J. Cryst. Growth **104**, 505 (1990).

[9] A. J. Ardell, in *Proceedings of the International Conference on Mechanism of Phase Transformation in Crystalline Solids, London, 1969*, Report No. 33 (The Institute of Metals, London, 1969), p. 111.

[10] O. Glatter and O. Kratky, *Small Angle X-ray Scattering* (Academic, London, 1982).